Review

Israel Journal of Chemistry
www.ijc.wiley-vch.de

doi.org/10.1002/ijch.202300022

The Mobility of Homomeric Lasso- and Daisy Chain-Like Rotaxanes in Solution and in the Gas Phase as a Means to Study Structure and Switching Behaviour

Adrian Saura-Sanmartin*[a, b] and Christoph A. Schalley[b]

This review is dedicated to Helmut Schwarz on the occasion of his 80th birthday

Abstract: A precise structural determination of supramolecular architectures is a non-trivial challenge. This daunting task can be made even more difficult when interlocked species are to be analysed having macrocycles covalently equipped with a thread as repeating units, such as molecular lassos and daisy chains. When such functionalized macrocycles are included as scaffolds, different products having analogous NMR spectra as well as dynamic libraries can be obtained. Furthermore, if control over the motion of the parts relative to each other is to be achieved, a full understanding of the machinery's operation mechanism requires detailed insight into the structures involved. This understanding also helps designing improved synthetic molecular machines. Diffusion-ordered NMR spectroscopy and ion-mobility MS techniques are ideal tools to study such compounds in depth. This review covers recent examples on the use of the above-mentioned techniques to characterize these interlocked architectures.

Keywords: diffusion NMR · ion mobility MS · rotaxanes · daisy chains · molecular lassos

1. Introduction

Mechanically interlocked molecules (MIMs) are compounds with at least two parts linked through non-covalent forces in a so-called mechanical bond.[1] This molecular architecture has been a hot topic within the research field of supramolecular chemistry in the last decades as a consequence of its application in molecular machinery.[2] New forms of catalysis[3] and chirality,[4] as well as the construction of interlocked materials,[5] among other applications, have been reported.

Rotaxanes,[6] molecules having at least one cyclic component, the wheel, threading a linear one, the axle, have been widely employed in the development of molecular machines due to the switchability and dynamic behaviour of their counterparts.[7,8] The operation of these intertwined molecules as nanomachines requires a rational design that is often inspired by biological systems.[9] Synthetic chemists have found inspiration in lassopeptides[10] and in the motion of sarcomeres[11] designing rotaxane-based molecular lassos[12] and [*c2*]daisy chains,[13] among higher order arrangements.[14] These interlocked compounds are usually synthesized starting from a cyclic molecule or cyclic precursor having a covalently attached thread, also known as the arm. The binding between the arm and the cavity of the cyclic part can lead to a library of different possibilities (Figure 1), including [1]rotaxanes, as well as different acyclic and cyclic daisy chains in which identical macrocycles mutually interlocked with each other through their arms.

The structural characterization of the possible interlocked products has an inherent difficulty, since many of them show very similar Nuclear Magnetic Resonance (NMR) spectra. A further complication exists in the case of pseudorotaxanes, when dynamic libraries are obtained or when changes in the position of the counterparts as a consequence of the intrinsic dynamics occur. As the different assemblies shown in Figure 1, however, differ in size, diffusion-ordered NMR spectroscopy (DOSY) and ion mobility mass spectrometry (IMMS) are ideal experiments to study these molecules. While DOSY-NMR experiments can also probe the dynamics of rearrangements between the different structures, when these rearrangement occur on a suitable time scale, IMMS experiments use gaseous ions, which have a relatively inert environment and

[a] *A. Saura-Sanmartin*
Departamento de Química Orgánica,
Facultad de Química,
Universidad de Murcia
Calle Campus Universitario, 5,
30100 Murcia, Spain
E-mail: adrian.saura@um.es
[b] *A. Saura-Sanmartin, C. A. Schalley*
Institut für Chemie und Biochemie
Freie Universität Berlin
Arnimallee 20, 14195 Berlin, Germany

Israel Journal of Chemistry

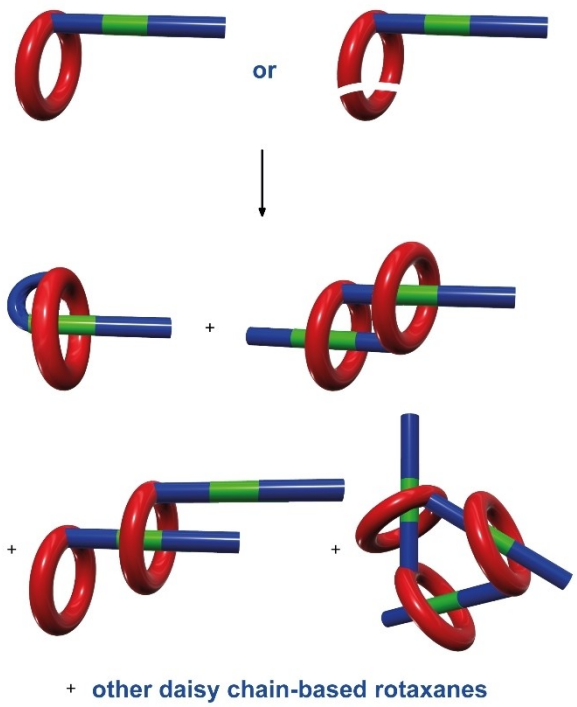

Figure 1. Synthesis of a library of rotaxane-based molecules starting from a precursor covalently equipped with a thread (template is shown in green).

thus do not undergo dynamic exchanges anymore. Both methods are thus nicely complementary to each other.

This short review focusses on the use of these techniques in the characterization of homomeric rotaxane-based molecular lassos and daisy chains. The manuscript is divided into two main sections, one section on the use of DOSY for that purpose and the other one on the use of IMMS. Both sections include a brief introduction to the technique and selected recent examples. In a final part, a critical perspective is provided.

Although examples combining both techniques exist in the literature, the use of mobility data from both techniques to structurally characterize this type of compounds is not common. The focus of this review could encourage a more frequent use of these analytical techniques for this purpose.

2. Diffusion ordered NMR Spectroscopy

The self-diffusion coefficient (D) is a quantitative measurement of the mobility of a molecule in solution and is dependent on the viscosity of the medium, as well as on the size and shape of the molecule. Intermolecular interactions affect this coefficient by varying the mobility of the molecule. These values can be determined by using pulsed-field gradient spin-echo (PGSE) NMR experiments. The DOSY technique shows the PGSE measurements as a two-dimensional spectrum in which the D values are displayed in one dimension and the chemical shifts in the other one. Thus, different species can be differentiated based on their molecular sizes.[14]

The Stokes-Einstein equation [Eq. (1)][15] is used to determine the molecular size information from diffusion coefficients measured in NMR. In this equation, k_B is the Boltzmann constant, T the absolute temperature, η the viscosity of the solvent and r_H the hydrodynamic radius of the molecule. This equation is valid for spherical particles and thus is only an approximation when molecules that deviate much from a sphere shape are studied.

$$D = \frac{k_B T}{6\pi\eta r_H} \tag{1}$$

The diffusion measurements also provide information of the molecular weight of the different aggregates in solution employing the equation stablished by Reinhoudt, Cohen and coworkers [Eq. (2)].[16] This equation assumes that the ratio of the diffusion coefficients of two different molecules (D_j/D_i) is inversely proportional to the cubic or square root of the ratio of their molecular weights (M_i/M_j), for spherical and rod-like species, respectively.

$$\sqrt[3]{\frac{M_i}{M_j}} \leq \frac{D_j}{D_i} \leq \sqrt[2]{\frac{M_i}{M_j}} \tag{2}$$

The DOSY technique, which has been widely used in supramolecular coordination chemistry,[14c] has turned out to be a valuable tool for the investigation of mechanically interlocked molecules as well, allowing to distinguish between

Adrian Saura-Sanmartin completed his PhD studies in 2021 at the Universidad de Murcia (Spain), working on rotaxanes under the supervision of Jose Berna and Alberto Martinez-Cuezva. In 2022, he joined the research group of Christoph Schalley at Freie Universitat Berlin (Germany) as a guest postdoctoral researcher. His research interests include the synthesis of interlocked molecules and their application for the preparation of smart materials.

Christoph A. Schalley carried out his PhD studies working on mass spectrometry and gas phase chemistry with Helmut Schwarz at Technical University Berlin. He worked on supramolecular chemistry as a postdoctoral researcher with Julius Rebek, Jr. In 2005, he was appointed professor of organic chemistry at Freie Universität Berlin (Germany). His research topics are diverse and comprise supramolecular chemistry in the gas phase as well as in solution and at interfaces.

species of different size and even analyze their machine-like motion on the basis of their shape.

2.1 Diffusion Coefficient as a Measurement of the Size

As mentioned above, the molecular size of a compound can be calculated from the *D* value using the Stokes Einstein equation.[15] This calculation is usually complemented by comparing with other molecules whose structures are well known or with computational models. Thus, the distinction between the different products which can be obtained through the reaction of a molecule covalently equipped with a thread is simplified, since their molecular formulas are *n* times that of the repeating unit, leading to a drastic size increase.

The DOSY technique was effectively used to analyze a series of daisy chain-type rotaxanes showing a muscle-like motion reported by Chiu and coworkers.[17] Compounds **1a–e** having pyridine-based macrocycles functionalized with bipyridine-based threads (Figure 2a) were reacted with $Zn(ClO_4)_2$ in a 1 : 1 ratio using CD_3CN as the solvent. The subsequent

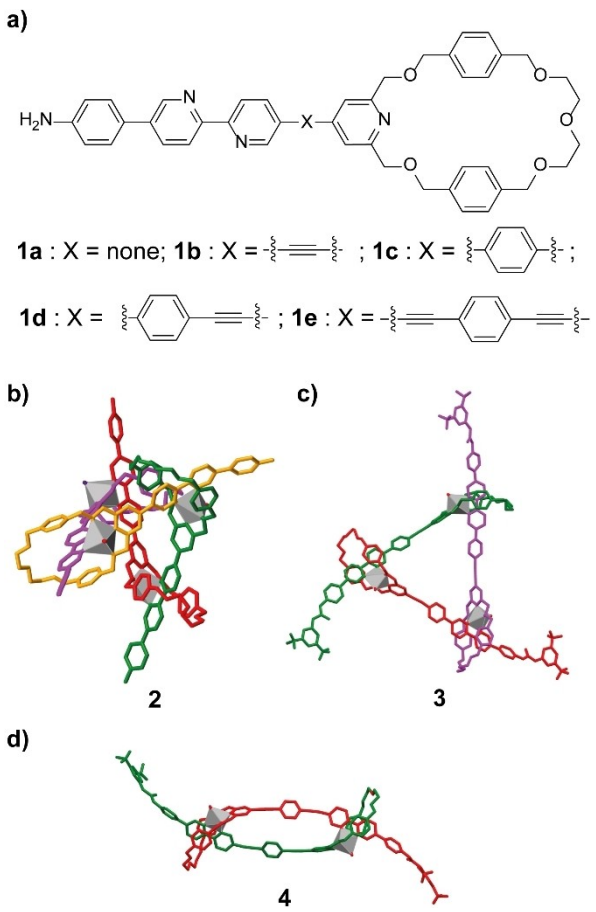

Figure 2. a) Chemical structures of compounds **1a–e**; and solid-state structures of: b) [*c4*]daisy chain **2**; c) [*c3*]daisy chain **3**; and d) [*c2*]daisy chain **4**.[17]

stoppering with 1-isocyanato-3,5-bis(trifluoromethyl)benzene afforded the corresponding daisy chain rotaxanes having urea as well as bipyridine stations. The reaction of **1a** and the zinc salt formed the quasi-tetrahedral [*c4*]daisy chain complex **2** as confirmed by X-ray crystallography (Figure 2b). When **1b–d** were employed, [*c3*]daisy chains emerged as the main products in accordance with the obtained larger *D* values in CD_3CN compared to that of **2**. This observation was confirmed after stoppering by the solid-state structure of [*c3*]daisy chain **3** obtained from **1b** (Figure 2c). Interestingly, when an equimolar solution of **1e** and Zn salt in CD_3CN was heated at 393 K for 96 hours, two species were obtained: a minor product which corresponds to the [*c3*]daisy chain as determined by the assistance of DOSY, and a major product showing a larger *D* value that can thus be assigned to the somewhat smaller [*c2*]daisy chain, whose structure was also confirmed by the X-ray crystallography after stoppering of crystals of the intertwined product **4** (Figure 2d). This example clearly illustrates the DOSY technique to be able to accurately identify the nature of the different daisy chains based on their size in nice agreement with the single-crystal structures.

The measurement of the *D* values was also used by Berna and coworkers in the characterization of a series of benzylic amide molecular lassos obtained from an acyclic U-shaped diamine precursor having a thread with two stations (fumaramide and succinamide-ester) through a clipping reaction. Only one type of interlocked compound was obtained, whose hydrodynamic radii as determined from the *D* values measured in $CDCl_3$ were in accordance with the sizes calculated from computational molecular models. Furthermore, the structure of one of the products, [1]rotaxane **5**, was confirmed by X-ray diffraction analysis (Figure 3a).[18] The same research group also made use of a strategy involving competitive self-templating clipping reactions which led to [*c2*]daisy chain **6** and the corresponding molecular lasso **7** (Figure 3b).[19] In this synthetic protocol, an unusual double clipping reaction of the diamine **8** and 5-(*tert*-butyl)isophthaloyl dichloride (**9**) competing with the molecular lasso formation was accomplished. The optimized conditions afforded a 1 : 1.4 ratio of **6** : **7**. The ^{1}H NMR spectra of **6** and **7** featuring similar pattern of signals and the deviation of the relative peak intensities in the high-resolution mass spectrometry (HRMS) complicated the structure assignment. Thus, the DOSY technique was crucial to unambiguously determine the structure of these intertwined polyamides. The *D* value of **7** is 5.04×10^{-10} m^2 s^{-1}, really close to the value of **5**, suggesting a lasso-like structure of this interlocked compound. The diffusion coefficient decreases to 3.74×10^{-10} m^2 s^{-1} in compound **6**, indicating a larger size. The ratio between the *D* values of **7** and **6** is 1.35 which matches to an approximate 1 : 2 mass ratio, thus supporting the formation of a [*c2*]daisy chain. The hydrodynamic radius of **7** (7.8 Å) was in agreement with that calculated from the solid-state structure of [1]rotaxane **5**. The higher value for **6** (10.5 Å) was in agreement with that calculated from a modeled structure (9.1 Å). The small differences of these two values can be

Israel Journal of Chemistry

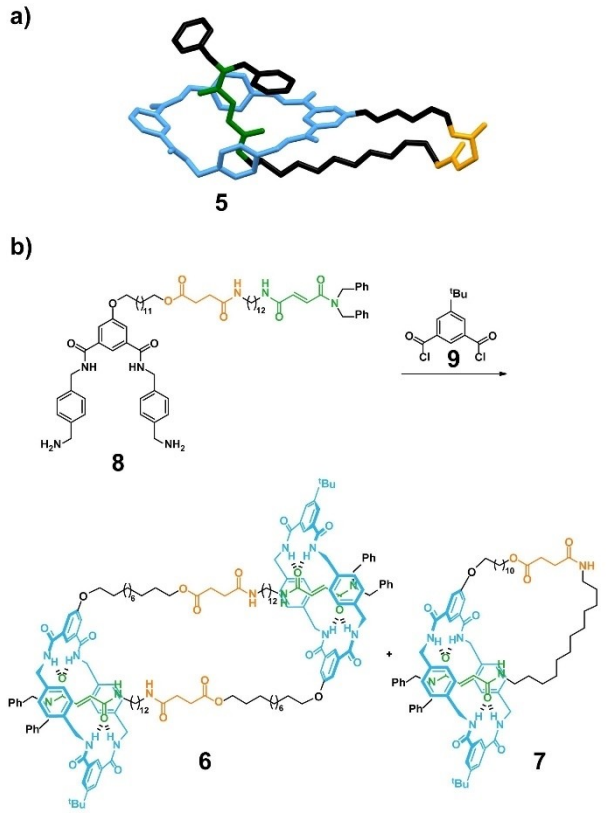

Figure 3. a) X-ray crystal structure of molecular lasso **5**;[18] and b) synthesis of [*c2*]daisy chain **6** and molecular lasso **7** through competitive self-templating clipping reactions.[19]

attributed to the hollow and elongated shape of the [*c2*]daisy chain together with solvation effects.

Stoddart and colleagues reported the synthesis of the [*c3*]daisy chains **10a,b** employing radical and cationic templates (Figure 4).[20] These intertwined architectures are assembled from repeating monomers of a cyclobis(paraquat-*p*-phenylene) (CBPQT) macrocycle bearing a thread decorated with a bipyridinium unit and a triazole ring. The hydrodynamic diameters of these interlocked compounds (3.34 nm and 4.17 nm) calculated using ^{1}H DOSY NMR were in fairly good agreement with the simulated molecular sizes using DFT-optimized geometries (3.6 nm and 4.9 nm).

2.2 Diffusion Coefficient as a Measurement of the Shape

The mobility of a molecule in solution is also affected by the molecular shape.[14] Thus, the motion of the counterparts of the interlocked products which can be controlled by the application of external stimuli leads to a variation in their diffusion coefficients.

In the last decade, two research groups have reported the synthesis of a double-lasso macrocycle starting from a [*c2*]daisy chain rotaxane,[21,22] in which the conversion between

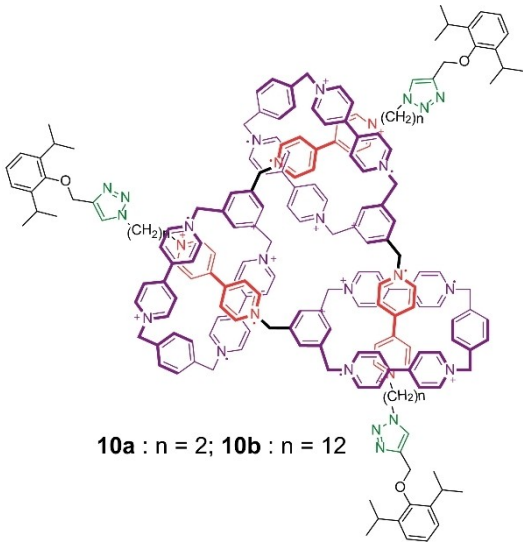

Figure 4. Chemical structure of **10a,b**.[20]

extended and contracted isomers was studied by DOSY experiments. In the example of Qu and coworkers, the shrinkable double-lasso macrocycle **11a** was prepared from a crown ether-based [*c2*]daisy chain rotaxane in which both thread motifs are connected through a coumarin unit (Figure 5).[22] In the contracted form, the macrocycles reside on the ammonium stations. Deprotonation using 1,8-diazabicyclo[5.4.0]undec-7-ene (DBU) afforded the extended isomer **11b**, in which the macrocycles encircle the imidazolium stations. Protonation with trifluoroacetic acid (TFA) restores the initial state of the system. This reversible motion was studied by ^{1}H NMR DOSY measurements using CD_3CN as solvent, determining a D value of 1.85×10^{-9} m^2 s^{-1} for **11a**, and 1.01×10^{-9} m^2 s^{-1} for **11b**. These values confirmed the smaller size of **11a** having a faster mobility than that of **11b** due to the different compaction.

Evans and coworkers also employed the DOSY technique to differentiate between two species which are only distinguishable from each other by the existence or absence of a mechanical bond, [1]rotaxane **12** and macrocycle **13**.[23] The D values measured in DMSO-d_6 were 1.28×10^{-10} m^2 s^{-1} for **12** (Figure 6a) and 1.10×10^{-10} m^2 s^{-1} for **13** (Figure 6b), which are in fully good agreement with the DFT simulated structures of the monomeric intertwined and non-intertwined forms. The higher D value obtained for the interlocked product compared to that of the non-interlocked one indicates a more compact tridimensional structure in solution, being consistent with the existence of a mechanical bond. Thus, the DOSY technique can be employed in order to determine the presence of such a bond when both interlocked and non-interlocked analogous are available.

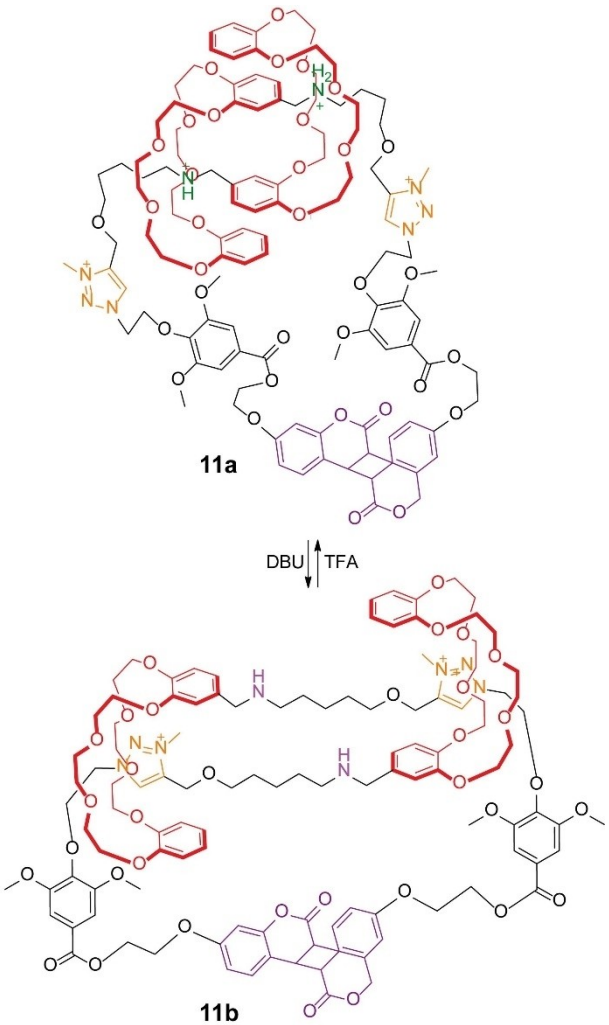

Figure 5. Exchange of the extended and contracted forms of double-lasso macrocycle **11**.[22]

3. Ion Mobility MS

Ion mobility mass spectrometry is a technique which provides very precise information regarding size and shape of ions in the gas phase as a consequence of their mobility in a drift tube filled with a collision gas.[24] The ions are first separated through a carrier gas depending on their mobility in the drift tube and then detected in a conventional mass analyzer according to their arrival times. As ions of different sizes undergo a different number of collisions and are thus retarded to different velocities and different arrival times, the distinction of ions with the same *m/z* ratio, but different sizes is possible.

Collision cross section (CCS) values can be determined from the arrival times as a molecular property independent of the instrument used and provide information of the shape and size of the ions in the gas phase. Compact or spherical molecules have small values of CCS, while extended molecules show higher values.[25] Collision cross sections can also be calculated from structural models by different methods. The comparison of theoretical and experimental cross sections is a good way to rule out certain isomers and to confirm a structure assignment.

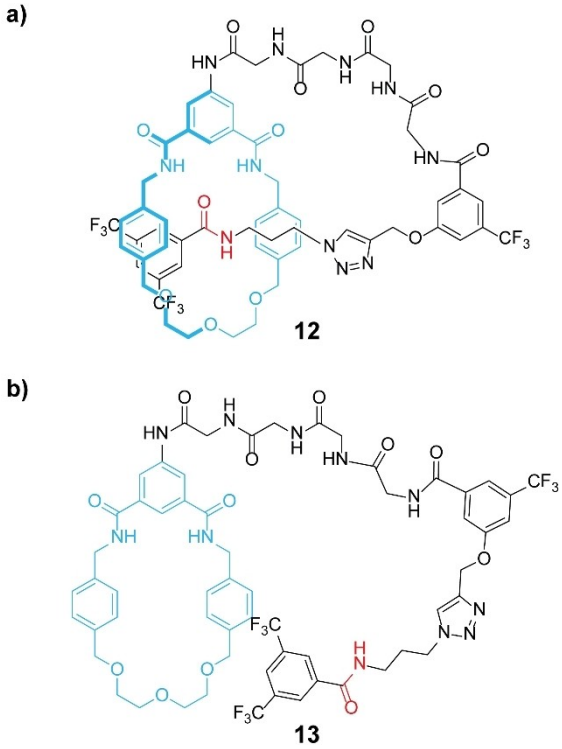

Figure 6. Chemical structure of: a) [1]rotaxane **12**; and b) macrocycle **13**.[23]

The Mason-Schamp equation [Eq. (3)][26] is used to calculate CCS values. In this equation, Ω is the integrated CCS, e the elementary charge, z the ion charge state, t_d the drift time, E the magnitude of the electric field, μ the reduced mass of the drift gas and the ion, k_B the constant of Boltzmann, T the temperature of the gas, L the length of the drift tube and N the number density of the buffer gas.

$$\Omega = \frac{3}{16}\left(\frac{2\pi}{(\mu k_B T)}\right)^{\frac{1}{2}}\frac{ezEt_d}{LN} \qquad (3)$$

Ion mobility MS has become a highly valuable tool in order to analyze supramolecular complexes,[27] and has also been successfully employed to determine the topology of different interlocked and knotted compounds.[28,29]

Although less frequently used than DOSY, this spectrometric technique should be included in the analytical toolbox to characterize lasso- and daisy chain-like rotaxanated architectures.

The study of the light driven exchange between [*c2*]daisy chain- and lasso-like isomers of a crown ether-based pseudo-

[1]rotaxane by IMMS was recently reported.[30] For this purpose, the heteroditopic monomer *E*-**14**, in which a crown ether is connected to a secondary ammonium station through an arylazopyrazole (AAP) spacer with *E* configuration (Figure 7), is dissolved in CD_3CN, leading to an equilibrium between this monomer and the [*c2*]daisy chain *E*,*E*-**15**. Upon light irradiation at 365 nm, the photoisomerization of the AAP motif was carried out, affording *Z*-**14** which was in equilibrium with the molecular lasso *Z*-**16**. Interestingly, the formation of intertwined species was favoured in both equilibria. Irradiation at 530 nm restored the initial conditions of the system. IMMS was employed to determine the switching mechanism in the gas phase. A peak having a drift time of 8.6 ms is observed in the mobilogram before irradiation. The *m*/z value of 654 having a peak spacing of 0.5 suggests the formation of *E*,*E*-**15**. When irradiating at 365 nm for 5 minutes, a decreasing in intensity for this dimer is observed and two new main peaks appear at 8.4 ms and 10.9 ms. The drift time of 8.4 ms corresponds to a doubly charged ion while the one at 10.9 ms is singly charged and can thus be attributed to *Z*-**16**. Increasing irradiation time finally makes the ions at 10.9 ms arrival time the main product, along with only traces of the doubly charged species. The peak at 8.4 ms suggests the formation of an intermediate [*c2*]daisy chain having an *E*,*Z* configuration (*E*,*Z*-**15**) whose subsequent isomerization and disassembly led to the pseudo[1]rotaxane product *Z*-**16**. The reverse isomerization process was also studied, observing the reassembly of the dimeric species *E*,*E*-**15**. Theoretical CCS values (467 $Å^2$, 462 $Å^2$ and 278 $Å^2$ for *E*,*E*-**15**, *E*,*Z*-**15** and *Z*-**16**, respectively) and PM6 level calculations supported the proposed switching mechanism.

Although the example discussed below was reported prior to the above-mentioned work, it has been selected as the last example, as it may serve as an interesting example for the complementary application of both IMMS and DOSY to obtain complementary structural data.

The reversible dethreading of the lasso-like pseudo[1]rotaxane **17**, a crown ether macrocycle carrying a naphthalene and a tetrathiafulvalene (TTF) unit and connected to an alkyl benzyl ammonium side chain, was recently studied using this spectrometric technique (Figure 8).[31] The two $1e^-$ oxidations experienced by the TTF scaffold led to three different charge states that were identified in the mass spectra (neutral TTF: +1; $TTF^{+\bullet}$: +2 and TTF^{2+}: +3). The oxidation of the TTF unit led to the dethreading of the pseudorotaxane while the reduction reestablished the pseudorotaxane structure. The researchers employed travelling wave ion mobility MS[32] in order to study the redox-switchable behavior of **17** using different trap voltages. Two peaks showing drift times of 9.45 ms and 10.25 ms were detected for the different isomers for the lower charge state (neutral TTF: +1). Both threaded and non-threaded isomers were observed for the different charge states, since two peaks were always detected, observing an increase in the intensity of the peak having the lower drift time at higher oxidation states. Interestingly, as the dethreading process is most favoured in the most oxidized state as a consequence of the repulsion of the benzyl alkyl ammonium arm induced by the dicationic TTF aromatic-aromatic interactions with the naphthalene motif, the smaller drift time was thus attributed to the non-threaded species, which is rather unusual. This conclusion was confirmed by collision-induced dissociation (CID) experiments, observing a predominance of the non-threaded species (lower drift time) by increasing the

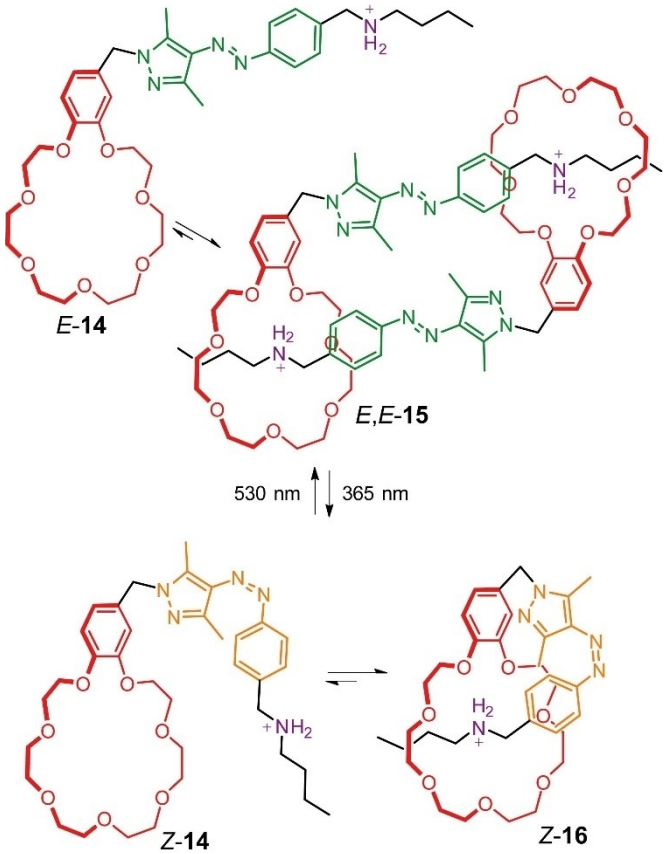

Figure 7. Photoswitchable exchange between [*c2*]-daisy chain *E*,*E*-**15** and molecular lasso *Z*-**16**.[30]

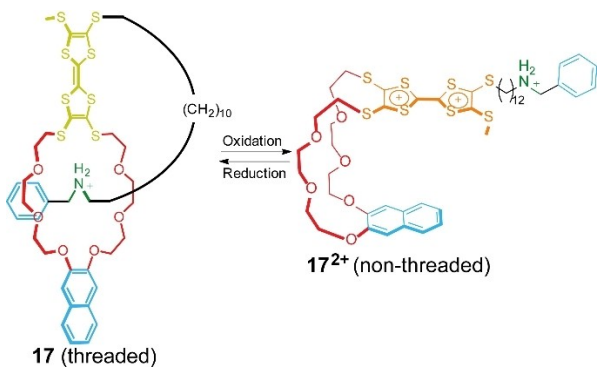

Figure 8. Redox-controlled switching of **17** showing the lowest and the highest oxidation states.[31]

collision energy, thus concluding that the crown ether must fold in the empty state. These results are complemented with those observed in cyclic voltammetry, confirming the switching process both in solution and in the gas phase. In this work, the DOSY technique was also employed, observing only a set of signals for **17** in CD_2Cl_2 in the DOSY spectrum, with a diffusion coefficient value of 7.43 $m^2 s^{-1}$, which corresponds to a hydrodynamic radius of 0.70 nm. This value is in accordance with the structure of the pseudo[1]rotaxane, thus excluding the formation of other oligomeric species, such as linear or cyclic daisy chains. Here, both techniques address different structural aspects: DOSY confirms the threaded nature of the initial, non-oxidized lasso pseudorotaxane, while IMMS is capable of characterizing the different switching states upon oxidation of the TTF.

4. Summary and Outlook

The measurement of the mobility of interlocked molecules in solution or in ionized form in the gas phase has been shown to be a structural identifier, providing information related to size, shape and topology. Thus, DOSY and IMMS have facilitated the unambiguous structural characterization of complex molecular architecture, such as homomeric molecular lassos and daisy chains. In addition to structural information, these instrumental techniques have been employed to monitor the operation of these rotaxanated systems as molecular machines.

Although the DOSY NMR technique has been used more frequently than IMMS, both provide complementary information and should be included to the instrumental toolbox for studying lasso- and daisy chain-like rotaxanes. These techniques provide useful information that leads to the distinction of different interlocked products having a macrocycle covalently equipped with a thread as repeating unit. Furthermore, the subtlety of the provided data allows the discrimination between species having the same molecular weight, such as conformational isomers, threaded and non-threaded species or cyclic and acyclic daisy chains. Complementary analyses are required in order to extract this information, including other NMR and MS experiments, as well as computational calculations.

In particular for IMMS experiments, very small amounts of sample are needed, which is especially relevant because of the synthetic difficulty of many of these interlocked systems along with the low yields obtained for some of the synthesized products. Additionally, in the case of DOSY experiments, the sample can be recovered after the measurement.

Both techniques of course also have their limitations. The mobility of molecules in solution is influenced by other factors, such as solvation and concentration, affecting the diffusion coefficient values. Regarding ion mobility MS, the structural changes which can occur during ionization and desolvation should be taken into account. The comparison of the data obtained from both techniques is necessary in order to increase their reliability.

DOSY and IMMS are related to each other, since both determine mobility data. The drift of the ions in the gas phase through the collision gas is an analogue of the medium where diffusion occurs in solution. Despite these similarities, both analytical techniques have differences. When fast exchanges occur on the DOSY time scale, the data interpretation is more difficult, but at the same time, the possibility to study such dynamic processes on the right time scale is a useful tool. In the case of IMMS, all exchanges except intramolecular ones are suppressed since the mobility of gaseous ions, which are separated particles, is measured. Thus, IMMS allows to freeze situations in which fast exchanges in solution complicate the bigger picture. Therefore, complementary information on the system under study is obtained when both techniques are employed.

These techniques nevertheless significantly facilitate the determination of the molecular structure when single crystal X-ray diffraction data are not available. Furthermore, the study of the switching mechanism of these molecular architectures is simplified considering the mobility of the different species. For this reason, the combination of both measurements is expected to become routine in the analysis of rotaxane-based molecular lassos and daisy chains.

Acknowledgements

This work was funded by the European Union – NextGenerationEU (Margarita Salas postdoctoral grant, Ministerio de Universidades of the Government of Spain) and the Deutsche Forschungsgemeinschaft (DFG; project number 434455294). Although the primary affiliation of Adrian Saura-Sanmartin is Universidad de Murcia, the author is currently a Margarita Salas guest postdoctoral researcher at Freie Universität Berlin since January 2022 (until December 2023). All figures included in this manuscript are original and have been redrawn based on the content of the referenced research articles by using: (i) FAIR open data from X-ray structures and Mercury® 2020.1 Software (Cambridge Crystallographic Data Center); (ii) chemical structures employing ChemBioDraw® Ultra 12.0 (CambridgeSoft, PerkinElmer Inf.); (iii) cartoon representations employing Autodesk 123D® (Autodesk Inc.) and Adobe Illustrator® (Adobe Inc.). A.S.-S. thanks Aurelia Pastor for introducing him to NMR diffusion experiments during his PhD studies and Andreas Springer for the training in the use of the ion mobility MS apparatus.

References

[1] a) C. J. Bruns, J. F. Stoddart, *The Nature of the Mechanical Bond: From Molecules to Machines*, Wiley-VCH, Weinheim, **2016**; b) J. F. Stoddart, *Angew. Chem. Int. Ed.* **2017**, *56*, 11094–11125; *Angew. Chem.* **2017**, *129*, 11244–11277; c) A. W. Heard, S. M. Goldup, *ACS Cent. Sci.* **2020**, *6*, 117–128.

[2] a) S. Erbas-Cakmak, D. A. Leigh, C. T. McTernan, A. L. Nussbaumer, *Chem. Rev.* **2015**, *115*, 10081–10206; b) E. R. Kay, D. A. Leigh, *Angew. Chem. Int. Ed.* **2015**, *54*, 10080–10088; *Angew. Chem.* **2015**, *127*, 10218–10226; c) M. Baroncini, L. Casimiro, C. de Vet, J. Groppi, S. Silvi, A. Credi, *ChemistryOpen* **2018**, *7*, 169–179; d) S. Krause, B. L. Feringa, *Nat. Chem. Rev.* **2020**, *4*, 550–562.

[3] a) L. van Dijk, M. J. Tilby, R. Szpera, O. A. Smith, H. A. P. Bunce, S. P. Fletcher, *Nat. Chem. Rev.* **2018**, *2*, 0117; b) A. Martinez-Cuezva, A. Saura-Sanmartin, M. Alajarin, J. Berna, *ACS Catal.* **2020**, *10*, 7719–7733; c) A. W. Heard, J. Meijide Suárez, S. M. Goldup, *Nat. Chem. Rev.* **2022**, *6*, 182–196.

[4] a) E. M. G. Jamieson, F. Modicom, S. M. Goldup, *Chem. Soc. Rev.* **2018**, *47*, 5266–5311; b) K. Nakazono, T. Takata, *Symmetry* **2020**, *12*, 144; c) J. R. J. Maynard, S. M. Goldup, *Chem* **2020**, *6*, 1914–1932.

[5] a) S. Mena-Hernando, E. M. Pérez, *Chem. Soc. Rev.* **2019**, *48*, 5016–5032; b) T. Takata, *ACS Cent. Sci.* **2020**, *6*, 129–143; c) B. H. Wilson, S. J. Loeb, *Chem* **2020**, *6*, 1604–1612; d) L. Chen, X. Sheng, G. Li, F. Huang, *Chem. Soc. Rev.* **2022**, *51*, 7046–7065; e) G. Liu, P. M. Rauscher, B. W. Rawe, M. M. Tranquilli, S. J. Rowan, *Chem. Soc. Rev.* **2022**, *51*, 4928–4948; f) A. Saura-Sanmartin, A. Pastor, A. Martinez-Cuezva, G. Cutillas-Font, M. Alajarin, J. Berna, *Chem. Soc. Rev.* **2022**, *51*, 4949–4976; g) J. S. W. Seale, Y. Feng, L. Feng, R. D. Astumian, J. F. Stoddart, *Chem. Soc. Rev.* **2022**, *51*, 8450–8475; h) A. López-Moreno, J. Villalva, E. M. Pérez, *Chem. Soc. Rev.* **2022**, *51*, 9433–9444.

[6] M. Xue, Y. Yang, X. Chi, X. Yan, F. Huang, *Chem. Rev.* **2015**, *115*, 7398–7501.

[7] Reviews on switchable rotaxanes: a) H. Tian, Q.-C. Wang, *Chem. Soc. Rev.* **2006**, *35*, 361–374; b) H. V. Schröder, C. A. Schalley, *Chem. Sci.* **2019**, *10*, 9626–9639; c) B. Yao, H. Sun, L. Yang, S. Wang, X. Liu, *Front. Chem.* **2022**, *9*, 832735.

[8] For examples of switchable rotaxanes: a) C. Gao, Z.-L. Luan, Q. Zhang, S. Yang, S.-J. Rao, D.-H. Qu, H. Tian, *Org. Lett.* **2017**, *19*, 1618–1621; b) Q.-W. Zhang, J. Zajíček, B. D. Smith, *Org. Lett.* **2018**, *20*, 2096–2099; c) A. Saura-Sanmartin, A. Martinez-Cuezva, D. Bautista, M. R. B. Marzari, M. A. P. Martins, M. Alajarin, J. Berna, *J. Am. Chem. Soc.* **2020**, *142*, 13442–13449; d) S. Borsley, D. A. Leigh, B. M. W. Roberts, *J. Am. Chem. Soc.* **2021**, *143*, 4414–4420; e) B. H. Wilson, L. M. Abdulla, R. W. Schurko, S. J. Loeb, *Chem. Sci.* **2021**, *12*, 3944–3951; f) G. Gholami, B. H. Wilson, K. Zhu, C. A. O'Keefe, R. W. Schurko, S. J. Loeb, *Faraday Discuss.* **2021**, *225*, 358–370; g) L. Feng, Y. Qiu, Q.-H. Guo, Z. Chen, J. S. W. Seale, K. He, K. Wu, Y. Feng, O. K. Farha, R. D. Astumian, J. F. Stoddart, *Science* **2021**, *374*, 1215–1221; h) M. Gaedke, H. Hupatz, H. V. Schröder, S. Suhr, K. F. Hoffmann, A. Valkonen, B. Sarkar, S. Riedel, K. Rissanen, C. A. Schalley, *Org. Chem. Front.* **2021**, *8*, 3659–3667; i) A. H. G. David, P. García-Cerezo, A. G. Campaña, F. Santoyo-González, V. Blanco, *Org. Chem. Front.* **2022**, *9*, 633–642; j) M. Gaedke, H. Hupatz, F. Witte, S. M. R. Rupf, C. Douglas, H. V. Schröder, L. Fischer, M. Malischewski, B. Paulus, C. A. Schalley, *Org. Chem. Front.* **2022**, *9*, 64–74; k) X. Li, A. H. G. David, L. Zhang, B. Song, Y. Jiao, D. Sluysmans, Y. Qiu, Y. Wu, X. Zhao, Y. Feng, L. Mosca, J. F. Stoddart, *J. Am. Chem. Soc.* **2022**, *144*, 3572–3579; l) Y.-P. Tang, Y.-E. Luo, J.-F. Xiang, Y.-M. He, Q.-H. Fan, *Angew. Chem. Int. Ed.* **2022**, *61*, e202200638.

[9] a) L. Zhang, V. Marcos, D. A. Leigh, *Proc. Natl. Acad. Sci. USA* **2018**, *115*, 9397–9404; b) M. N. Tasbas, E. Sahin, S. Erbas-Cakmak, *Coord. Chem. Rev.* **2021**, *443*, 214039.

[10] H. Martin-Gómez, J. Tulla-Puche, *Org. Biomol. Chem.* **2018**, *16*, 5065–5080.

[11] a) C. J. Bruns, J. F. Stoddart, *Acc. Chem. Res.* **2014**, *47*, 2186–2199; b) M. Gautel, K. Djinović-Carugo, *J. Exp. Biol.* **2016**, *219*, 135–145; c) A. Goujon, E. Moulin, G. Fuks, N. Giuseppone, *CCS Chem.* **2019**, *1*, 83–96.

[12] a) C. Reuter, A. Mohry, A. Sobanski, F. Vögtle, *Chem. Eur. J.* **2000**, *6*, 1674–1682; b) C. Clavel, C. Romuald, E. Brabet, F. Coutrot, *Chem. Eur. J.* **2013**, *19*, 2982–2989; c) Y. Wang, J. Sun, Z. Liu, M. S. Nassar, Y. Y. Botros, J. F. Stoddart, *Chem. Sci.* **2017**, *8*, 2562–2568; d) N. Pairault, A. Bessaguet, R. Barat, L. Frédéric, G. Pieters, J. Crassous, L. Opalisnki, S. Papot, *Chem. Sci.* **2021**, *12*, 2521–2526; e) H. V. Schröder, M. Stadlmeier, M. Wühr, A. J. Link, *Chem. Eur. J.* **2022**, *28*, e202103615; f) L. Ma, R. Tang, Y. Zhou, J. Bei, Y. Wang, T. Chen, C. Ou, Y. Han, C.-G. Yan, Y. Yao, *Chem. Commun.* **2022**, *58*, 8978–8981; g) X.-S. Du, Y. Han, C.-F. Chen, *Chem. Eur. J.* **2022**, *28*, e202104024.

[13] a) S.-H. Chiu, S. J. Rowan, S. J. Cantrill, J. F. Stoddart, A. J. P. White, D. J. Williams, *Chem. Commun.* **2002**, 2948–2949; b) F. Coutrot, C. Romuald, E. Busseron, *Org. Lett.* **2008**, *10*, 3741–3744; c) B. Zhang, S. Dong, J. Liu, F. Huang, *Org. Lett.* **2012**, *14*, 306–309; d) C. Romuald, G. Cazals, C. Enjalbal, F. Coutrot, *Org. Lett.* **2013**, *15*, 184–187; e) B. Zheng, F. Klautzsch, M. Xue, F. Huang, C. A. Schalley, *Org. Chem. Front.* **2014**, *1*, 532–540; f) A. Goujon, T. Lang, G. Mariani, E. Moulin, G. Fuks, J. Raya, E. Buhler, N. Giuseppone, *J. Am. Chem. Soc.* **2017**, *139*, 14825–14828; g) S. Ikejiri, Y. Takashima, M. Osaki, H. Yamaguchi, A. Harada, *J. Am. Chem. Soc.* **2018**, *140*, 17308–17315; h) Q. Zhang, S.-J. Rao, T. Xie, X. Li, T.-Y. Xu, D.-W. Li, D.-H. Qu, Y.-T. Long, H. Tian, *Chem* **2018**, *4*, 2670–2684; i) S.-J. Rao, Q. Zhang, X.-H. Ye, C. Gao, D.-H. Qu, *Chem. Asian J.* **2018**, *13*, 815–821; j) A. Wolf, J.-J. Cid, E. Moulin, F. Niess, G. Du, A. Goujon, E. Busseron, A. Ruff, S. Ludwigs, N. Giuseppone, *Eur. J. Org. Chem.* **2019**, 3421–3432; k) S. Tsuda, Y. Komai, S. Fujiwara, Y. Nishiyama, *Chem. Eur. J.* **2021**, *27*, 1966–1969; l) J. M. Van Raden, N. N. Jarenwattananon, L. N. Zakharov, R. Jasti, *Chem. Eur. J.* **2020**, *26*, 10205–10209; m) H. V. Schröder, Y. Zhang, A. J. Link, *Nat. Chem.* **2021**, *13*, 850–857.

[14] a) K. F. Morris, C. S. Johnson Jr., *J. Am. Chem. Soc.* **1992**, *114*, 3139–3141; b) H. Barjat, G. A. Morris, S. Smart, A. G. Swanson, S. C. R. Williams, *J. Magn. Reson.* **1995**, *108*, 170–172; c) A. Pastor, E. Martínez-Viviente, *Coord. Chem. Rev.* **2008**, *252*, 2314–2345; d) R. Evans, *Prog. Nucl. Magn. Reson. Spectrosc.* **2020**, *117*, 33–69; e) J. Guest, P. Kiraly, M. Nilsson, G. A. Morris, *Magn. Reson.* **2021**, *2*, 733–739.

[15] A. Einstein, *Teilchen. Ann. Phys.* **1905**, *332*, 549–560.

[16] P. Timmerman, J.-L. Weidmann, K. A. Jolliffe, L. J. Prins, D. N. Reinhoudt, S. Shinkai, L. Frish, Y. Cohen, *J. Chem. Soc. Perkin Trans. 2* **2000**, 2077–2089.

[17] J.-C. Chang, S.-H. Tseng, C.-C. Lai, Y.-H. Liu, S.-M. Peng, S.-H. Chiu, *Nat. Chem.* **2017**, *9*, 128–134.

[18] A. Saura-Sanmartin, A. Martinez-Cuezva, A. Pastor, D. Bautista, J. Berna, *Org. Biomol. Chem.* **2018**, *16*, 6980–6987.

[19] A. Saura-Sanmartin, A. Pastor, A. Martinez-Cuezva, J. Berna, *Chem. Commun.* **2022**, *58*, 290–293.

[20] K. Cai, B. Cui, B. Song, H. Wang, Y. Qiu, L. O. Jones, W. Liu, Y. Shi, S. Vemuri, D. Shen, T. Jiao, L. Zhang, H. Wu, H. Chen, Y. Jiao, Y. Wang, C. L. Stern, H. Li, G. C. Schatz, X. Li, J. F. Stoddart, *Chem* **2021**, *7*, 174–189.

[21] C. Romuald, A. Ardá, C. Clavel, J. Jiménez-Barbero, F. Coutrot, *Chem. Sci.* **2012**, *3*, 1851–1857.

[22] S.-J. Rao, X.-H. Ye, Q. Zhang, C. Gao, W.-Z. Wang, D.-H. Qu, *Asian J. Org. Chem.* **2018**, *7*, 902–905.

[23] M. J. Young, G. R. Akien, N. H. Evans, *Org. Biomol. Chem.* **2020**, *18*, 5203–5209.

[24] a) H. Borsdorf, G. A. Eiceman, *Appl. Spectrosc. Rev.* **2006**, *41*, 323–374; b) A. B. Kanu, P. Dwivedi, M. Tam, L. Matz, H. H. Hill Jr., *J. Mass Spectrom.* **2008**, *43*, 1–22; c) F. Lanucara, S. W. Holman, C. J. Gray, C. E. Eyers, *Nat. Chem.* **2014**, *6*, 281–294; d) K. Michelmann, J. A. Silveira, M. E. Ridgeway, M. A. Park, *Anal. Chem.* **2017**, *86*, 2107–216; e) J. N. Dodds, E. S. Baker, *J. Am. Soc. Mass Spectrom.* **2019**, *30*, 2185–2195.

[25] J. C. May, C. B. Morris, J. A. McLean, *Anal. Chem.* **2017**, *89*, 1032–1044.

[26] a) H. E. Revercomb, E. A. Mason, *Anal. Chem.* **1975**, *47*, 970–983; b) C. B. Hariharan, J. I. Baumbach, W. Vautz, *Anal. Chem.* **2010**, *82*, 427–431; c) V. Shrivastav, M. Nahin, C. J. Hogan, C. Larriba-Andaluz, *J. Am. Soc. Spectrom.* **2017**, *28*, 1540–1551.

[27] a) B. Baytekin, H. T. Baytekin, C. A. Schalley, *Org. Biomol. Chem.* **2006**, *4*, 2825–2841; b) L. Cera, C. A. Schalley, *Chem. Soc. Rev.* **2014**, *43*, 1800–1812; c) E. Kalenius, M. Groessl, K. Rissanen, *Nat. Rev.* **2019**, *3*, 4–14; d) L. Polewski, A. Springer, K. Pagel, C. A. Schalley, *Acc. Chem. Res.* **2021**, *54*, 2445–2456.

[28] K. J. D. Fouque, C. Afonso, S. Zirah, J. D. Hegemann, M. Zimmermann, M. A. Marahiel, S. Rebuffat, H. Lavanant, *Anal. Chem.* **2015**, *87*, 1166–1172.

[29] A. Kruve, K. Caprice, R. Lavendomme, J. M. Wollschläger, S. Schoder, H. V. Schröder, J. R. Nitschke, F. L. Cougnon, C. A. Schalley, *Angew. Chem. Int. Ed.* **2019**, *58*, 11324–11328; *Angew. Chem.* **2019**, *131*, 11446–11450.

[30] C.-W. Chu, D. L. Stares, C. A. Schalley, *Chem. Commun.* **2021**, *57*, 12317–12320.

[31] H. V. Schröder, J. M. Wollschläger, C. A. Schalley, *Chem. Commun.* **2017**, *53*, 9218–9221.

[32] a) K. Giles, J. P. Williams, I. Campuzano, *Rapid Commun. Mass Spectrom.* **2011**, *25*, 1559–1566; b) G. Paglia, G. Astarita, *Methods Mol. Biol.* **2019**, *1978*, 39–53.

Manuscript received: February 2, 2023
Revised manuscript received: February 22, 2023
Version of record online: March 14, 2023